Proceedings of DSCC2008
2008 ASME Dynamic Systems and Control Conference
October 20-22, 2008, Ann Arbor, Michigan, USA

DSCC2008-2222

NEURAL NETWORK CONTROL OF A ROBOT INTERACTING WITH AN UNCERTAIN HUNT-CROSSLEY VISCOELASTIC ENVIRONMENT

S. Bhasin*, **K. Dupree, P. M. Patre, and W. E. Dixon,**
Department of Mechanical and Aerospace Engineering
University of Florida, Gainesville
email: {sbhasin, kdupree, pmpatre, wdixon}@ufl.edu

ABSTRACT

The objective in this paper is to control a robot as it transitions from a non-contact to a contact state with an unactuated viscoelastic mass-spring system such that the mass-spring is regulated to a desired final position. A nonlinear Hunt-Crossley model, which is physically consistent with the real behavior of the system at contact, is used to represent the viscoelastic contact dynamics. A Neural Network feedforward term is used in the controller to estimate the environment uncertainties, which are not linear-in-parameters. The NN Lyapunov based controller is shown to guarantee uniformly ultimately bounded regulation of the system despite parametric and nonparametric uncertainties in the robot and the viscoelastic environment respectively. The proposed controller only depends on the position and velocity terms, and hence, obviates the need for measuring the impact force and acceleration. Further, the controller is continuous, and can be used for both non-contact and contact conditions.

1 Introduction

There is practical motivation to study robot contact with a viscoelastic environment because of the increasing applications involving human-robot interaction [1]- [3]. Modeling contact and compensating for its effects in a closed loop controller has been a focus of research over the last two decades.

To capture the physical effects during contact, researchers, over the years, have proposed many contact models, ranging from the simplest Hertz model [4] to the more complex Kelvin-Voigt [5] and impact pair model [6]. Hunt and Crossley [7] proposed a compliant contact model, which not only included both the stiffness and damping terms, but also eliminated the discontinuous impact forces at initial contact and separation, thus making it more suitable for robotic contact with soft environments. Because the model has been shown to better represent the physical nature of the energy transfer process at contact [8], it has found acceptance in the scientific community [8]- [11].

Given some model of the impact dynamics, another challenge is to develop a closed loop controller for a robot, as it transitions from a non-contact to contact state. The destabilizing impact forces and the uncertainty in the environment dynamics make it a complex control problem. A variety of techniques have been developed to control the robot motion in the presence of a contact transition [12]- [20].

In our previous efforts [17–19] to tackle this problem, we used a linear spring contact model to develop a controller for robot contact transition with a stiff environment. The contribution of the work was the development of a single continuous controller for both the non-contact and contact states of the robot. In our most recent work [20], we used a more general Hunt-Crossley contact model which also accounted for the energy dissipation at contact, and hence was suitable for viscoelastic contact. An adaptive control scheme was developed in [20] to account for linearly parameterizable uncertainty in the environment. However, the development in [20] assumed the knowledge of the local deformation of the material raised to the Hertzian compliance exponent, which is usually difficult to de-

*Address all correspondence to this author.

[1]This research is supported in part by the NSF CAREER AWARD 0547448, NSF SGER 0738091, AFOSR contract numbers F49620-03-1-0381 and F49620-03-1-0170, AFRL contract number FA4819-05-D-0011, Department of Energy URPR program grant number DE-FG04-86NE37967, and by research grant No. US-3715-05 from BARD, the United States - Israel Binational Agricultural Research and Development Fund.

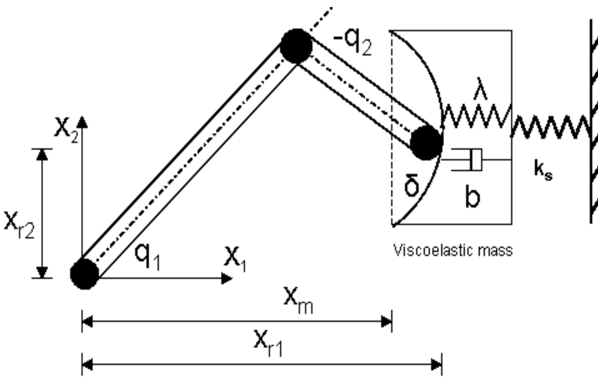

Figure 1. Robot contact with a viscoelastic mass.

termine [21]. One reason that exact knowledge of the Hertzian compliance exponent is required in [20] is that this effect is not linearly parameterizable.

In this paper, we use a Neural Network feedforward term in our controller to estimate the non linear-in-parameter (Non-LP) environment uncertainties. Thus, no knowledge of the environment parameters is required. In a recent work [22], an impedance control method in conjunction with an NN based environment estimation is used to generate reference trajectory for force tracking. However, accelerations and force measurements were used as inputs to the NN and the NN weights were tuned off-line. In this paper, only position and velocity measurements are required and no acceleration and force measurements are used in the design of the controller. Also, the NN weights are automatically adjusted online, with no off-line learning phase required. The control structure in this paper includes a desired robot velocity as a virtual control input to the unactuated viscoelastic mass-spring system, coupled with a force controller to ensure that the mass is regulated to the desired position. Uniformly Ultimately Bounded (UUB) stability of the controller is proven using Lyapunov stability analysis. An experimental testbed is currently being developed with a planar two-link direct drive robot that will collide with a viscoelastic human tissue phantom to test the performance of the developed controller.

2 Dynamic Model

The development in this paper is motivated by the academic problem illustrated in Fig. 1. While the subsequent control design and stability analysis is developed for a two degree-of-freedom (DOF) system in a planar Cartesian-space, the underlying mathematics can be extended to higher order systems without additional constraints. The dynamic model for a rigid two-link revolute robot in contact with a compliant viscoelastic environment is given by

$$M(x_r)\ddot{x}_r + C(x_r,\dot{x}_r)\dot{x}_r + h(x_r) + \begin{bmatrix} F_m \\ 0 \end{bmatrix} = F \tag{1}$$

$$m\ddot{x}_m + k_s(x_m - x_0) = F_m. \tag{2}$$

In (1), $x_r(t)$, $\dot{x}_r(t)$, $\ddot{x}_r(t) \in \mathbb{R}^2$ represent the planar Cartesian position, velocity, and acceleration of the robot links respectively, $M(x_r) \in \mathbb{R}^{2\times 2}$ represents the uncertain inertia matrix, $C(x_r,\dot{x}_r) \in \mathbb{R}^{2\times 2}$ represents the uncertain Centripetal-Coriolis effects, $h(x_r) \in \mathbb{R}^2$ represents uncertain conservative forces (e.g., gravity), $F_m(x_r,\dot{x}_r,x_m,\dot{x}_m) \in \mathbb{R}$ denotes the interaction force between the robot and the mass during impact, and $F(t) \in \mathbb{R}^2$ represents the force control inputs. In (2), $x_m(t)$, $\ddot{x}_m(t) \in \mathbb{R}$ represent the displacement and acceleration of the unknown viscoelastic mass $m \in \mathbb{R}$, $x_0 \in \mathbb{R}$ represents the initial undisturbed position of the mass, and $k_s \in \mathbb{R}$ represents the unknown stiffness of the spring connected to the mass. When the horizontal position of the robot, denoted by $x_{r1}(t) \in \mathbb{R}$, is greater than or equal to the position of the viscoelastic material (i.e., when $x_{r1}(t) \geq x_m(t)$, see Fig. (1)) contact occurs, and the interaction force $F_m(x_{r1},\dot{x}_{r1},x_m,\dot{x}_m)$ is modeled as

$$F_m = \Lambda F_v, \tag{3}$$

where $\Lambda(x_{r1},x_m) \in \mathbb{R}$ is a discontinuous function which switches at impact defined as

$$\Lambda \triangleq \begin{cases} 0 & x_{r1} < x_m \\ 1 & x_{r1} \geq x_m, \end{cases} \tag{4}$$

and $F_v(x_{r1},\dot{x}_{r1},x_m,\dot{x}_m) \in \mathbb{R}$ denotes the Hunt-Crossley force defined as [7]

$$F_v \triangleq \lambda\delta^n + b\dot{\delta}\delta^n. \tag{5}$$

In (5), $\lambda \in \mathbb{R}$ is the unknown contact stiffness of the viscoelastic mass, $b \in \mathbb{R}$ is the unknown impact damping coefficient, $\delta(x_r,x_m) \in \mathbb{R}$ denotes the local deformation of the material and is defined as

$$\delta \triangleq x_{r1} - x_m. \tag{6}$$

Also, in (5), $\dot{\delta}(t)$ is the relative velocity of the contacting bodies, and $n \in \mathbb{R}$ is the unknown Hertzian compliance coefficient which depends on the surface geometry of contact. The model in (3) is a continuous contact force-based model wherein the contact forces increase from zero upon impact and return to zero upon separation. Also, the energy dissipation during impact is a function of the damping constant which can be related to the impact velocity and the coefficient of restitution [7], thus making the model consistent with the physics of contact. The contact is considered to be direct-central and quasi-static (i.e., all the stresses are transmitted at the time of contact and sliding and friction effects during contact are negligible) where plastic deformation effects are assumed to be negligible.

The dynamic model in (1)-(5) exhibits the following properties that will be utilized in the subsequent analysis.

Property 1: The inertia matrix $M(x_r)$ is symmetric, positive definite, and can be lower and upper bounded as

$$a_1 ||\xi||^2 \leq \xi^T M \xi \leq a_2 ||\xi||^2, \qquad \forall \xi \in \mathbb{R}^2 \tag{7}$$

where $a_1, a_2 \in \mathbb{R}$ are positive constants and $\|\cdot\|$ denotes the standard Euclidean norm.

Property 2: The following skew-symmetric relationship is satisfied

$$\xi^T (\frac{1}{2}\dot{M}(x_r) - C(x_r, \dot{x}_r))\xi = 0 \qquad \forall \xi \in \mathbb{R}^2. \tag{8}$$

Property 3: The expression for the interaction force $F_m(x_r, \dot{x}_r, x_m, \dot{x}_m)$ in (3) can be written, using (4) and (6), as

$$F_m = \begin{cases} 0 & \delta < 0 \\ \lambda \delta^n + b\dot{\delta}\delta^n & \delta \geq 0. \end{cases} \tag{9}$$

Based on the fact that

$$\lim_{\delta \to 0^-} F_m = \lim_{\delta \to 0^+} F_m = 0, \tag{10}$$

the interaction force F_m is continuous.

Assumption 1: The robot and mass spring positions, $x_r(t)$ and $x_m(t)$, and the corresponding velocities, $\dot{x}_r(t)$ and $\dot{x}_m(t)$, are measurable. Further, it is assumed that the $x_r(t)$ and $x_m(t)$ are bounded. The bound on $x_r(t)$ is based on the geometry of the robot, and the bound on $x_m(t)$ is based on the physical fact that the mass is attached by the spring to some object, and the mass will not be able to move past that object.

Assumption 2: The local deformation of the viscoelastic material during contact, $\delta(x_r, x_m)$, defined in (6), is assumed to be upper bounded, and hence δ^n can be upper bounded as

$$\delta^n \leq \mu, \tag{11}$$

where $\mu \in \mathbb{R}$ is a positive bounding constant.

Assumption 3: We assume that the mass and the damping constant can be bounded as

$$\underline{m} \leq m \leq \overline{m} \qquad b \leq \overline{b} \tag{12}$$

where $\underline{m}$, $\overline{m}, \overline{b} \in \mathbb{R}$ denote known positive bounding constants.

3 Control Development

In the subsequent control development, the desired robot velocity is designed as a virtual control input to the unactuated viscoelastic mass, to ensure that the robot impacts and then regulates the mass to a desired position. Since it is not possible to directly control the mass trajectory, backstepping methods are then used to develop a lyapunov based NN controller to ensure that the robot tracks the desired trajectory despite the non-contact to contact transition and parametric uncertainties in the robot and non-parametric uncertainties in the viscoelastic mass-spring system. The viscoelastic model requires that the backstepping error be developed in terms of the desired robot velocity. A challenge to backstep on the desired robot velocity is that the desired velocity is premultiplied by $\Lambda(x_{r1}, x_m)$, which is zero when the robot and material are not in contact. Hence, a strategic combination of nonlinear damping and NN backstepping is used in the subsequent development.

3.1 Control Objective

The control objective is to regulate the position of a viscoelastic mass attached to a spring via a two-link planar robot that transitions from non-contact to contact with the mass-spring assembly through an impact collision. To quantify the control objective, the following errors are defined

$$e_r \triangleq x_{rd} - x_r \qquad e_m \triangleq x_{md} - x_m, \tag{13}$$

where $e_r(t) \triangleq [e_{r1}(t), e_{r2}(t)]^T \in \mathbb{R}^2$ and $e_m(t) \in \mathbb{R}$ denote the errors for the end-point of the second link of the robot and mass-spring system (MSR) (see Fig. 1), respectively. In (13), $x_{md} \in \mathbb{R}$ denotes the constant known desired position of the mass, and $x_{rd}(t) \triangleq [x_{rd1}(t), x_{rd2}]^T \in \mathbb{R}^2$ denotes the desired position of the end-point of the second link of the robot. To facilitate the subsequent control design and stability analysis, filtered tracking errors for the robot and the mass-spring, denoted by $r_r(t) \in \mathbb{R}^2$ and $r_m(t) \in \mathbb{R}$ respectively, are defined as

$$\begin{aligned} r_r &\triangleq \dot{e}_r + \alpha e_r \\ r_m &\triangleq \dot{e}_m + \gamma_1 e_m + \gamma_2 e_f, \end{aligned} \tag{14}$$

where $\alpha \in \mathbb{R}^{2\times 2}$ is a positive, diagonal, constant gain matrix, γ_1, $\gamma_2 \in \mathbb{R}$ are positive constant gains and $e_f(t) \in \mathbb{R}$ is an auxiliary filter variable designed as.

$$\dot{e}_f = -\gamma_3 e_f + \gamma_2 e_m - k_1 r_m, \tag{15}$$

where k_1, $\gamma_3 \in \mathbb{R}$ are positive constant control gains.

3.2 NN Feedforward Estimation

NN-based estimation methods are well suited for control systems where the dynamic model contains uncertainties as in (1), (2) and (5). The universal approximation Property of the Neural Network lends itself nicely to control system design.

Multilayer Neural Networks have been shown to be capable of approximating generic nonlinear continuous functions. Let $\mathbb{S}$ be a compact simply connected set of $\mathbb{R}^{N_1+1}$. With map $f : \mathbb{S} \to \mathbb{R}^n$, define $\mathbb{C}^n(\mathbb{S})$ as the space where f is continuous. There exist weights and thresholds such that some function $f(x) \in \mathbb{C}^n(\mathbb{S})$ can be represented by a three-layer NN as [23], [24]

$$f(x) = W^T \sigma\left(V^T x\right) + \varepsilon(x), \tag{16}$$

for some given input $x(t) \in \mathbb{R}^{N_1+1}$. In (16), $V \in \mathbb{R}^{(N_1+1)\times N_2}$ and $W \in \mathbb{R}^{(N_2+1)\times n}$ are bounded constant ideal weight matrices for the first-to-second and second-to-third layers respectively, where N_1 is the number of neurons in the input layer, N_2 is the number of neurons in the hidden layer, and n is the number of neurons in the third layer. The activation function in (16) is denoted by $\sigma(\cdot) \in \mathbb{R}^{N_2+1}$, and $\varepsilon(x) \in \mathbb{R}^n$ is the functional reconstruction error. Note that, augmenting the input vector $x(t)$ and activation function $\sigma(\cdot)$ by "1" allows us to have thresholds as the first columns of the weight matrices [23], [24]. Thus, any tuning of W and V then includes tuning of thresholds as well. The computing power of the NN comes from the fact that the activation function $\sigma(\cdot)$ is nonlinear and the weights W and V can be modified or tuned through some learning procedure [24]. Based on (16), the typical three-layer NN approximation for $f(x)$ is given as [23], [24]

$$\hat{f}(x) \triangleq \hat{W}^T \sigma(\hat{V}^T x), \tag{17}$$

where $\hat{V}(t) \in \mathbb{R}^{(N_1+1)\times N_2}$ and $\hat{W}(t) \in \mathbb{R}^{(N_2+1)\times n}$ are subsequently designed estimates of the ideal weight matrices. The estimate mismatch for the ideal weight matrices, denoted by $\tilde{V}(t) \in \mathbb{R}^{(N_1+1)\times N_2}$ and $\tilde{W}(t) \in \mathbb{R}^{(N_2+1)\times n}$, are defined as

$$\tilde{V} \triangleq V - \hat{V}, \quad \tilde{W} \triangleq W - \hat{W},$$

and the mismatch for the hidden-layer output error for a given $x(t)$, denoted by $\tilde{\sigma}(x) \in \mathbb{R}^{N_2+1}$, is defined as

$$\tilde{\sigma} \triangleq \sigma - \hat{\sigma} = \sigma(V^T x) - \sigma(\hat{V}^T x). \tag{18}$$

The NN estimate has several properties that facilitate the subsequent development. These properties are described as follows.

Property 5: (*Taylor Series Approximation*) The Taylor series expansion for $\sigma\left(V^T x\right)$ for a given x may be written as [23], [24]

$$\sigma(V^T x) = \sigma(\hat{V}^T x) + \sigma'(\hat{V}^T x)\tilde{V}^T x + O(\tilde{V}^T x)^2, \tag{19}$$

where $\sigma'(\hat{V}^T x) \equiv d\sigma\left(V^T x\right)/d\left(V^T x\right)|_{V^T x = \hat{V}^T x}$, and $O(\hat{V}^T x)^2$ denotes the higher order terms. After substituting (19) into (18) the following expression can be obtained:

$$\tilde{\sigma} = \hat{\sigma}' \tilde{V}^T x + O(\tilde{V}^T x)^2, \tag{20}$$

where $\hat{\sigma}' \triangleq \sigma'(\hat{V}^T x)$.

Property 6: (*Boundedness of the Ideal Weights*) The ideal weights are assumed to exist and be bounded by known positive values so that

$$\|V\|_F^2 \leq \bar{V}_B \quad and \quad \|W\|_F^2 \leq \bar{W}_B, \tag{21}$$

where $\|\cdot\|_F$ is the Frobenius norm of a matrix, and $tr(\cdot)$ is the trace of a matrix.

Property 7: (*Projection bounds for Weight Estimates)* The estimates for NN weights, $\hat{W}(t)$ and $\hat{V}(t)$, can be bounded using the projection algorithm as in [26].

Property 8: (*Boundedness of activation function* σ and $\dot{\sigma}$) The typical choice of activation function is the sigmoid function

$$\sigma(z) = \frac{1}{1+e^{\kappa z}}, \tag{22}$$

where

$$\|\sigma\| < 1 \text{ and } \|\dot{\sigma}\| \leq \sigma_n,$$

where $\sigma_n \in \mathbb{R}$ is a known positive constant.

Property 9: (*Boundedness of functional reconstruction error* $\varepsilon(x)$) On a given compact set S, the net reconstruction error $\varepsilon(x)$ is bounded as

$$\|\varepsilon(x)\| \leq \varepsilon_n,$$

where ε_n is a known positive constant.

Property 10: (*Property of trace*) If $A \in \mathbb{R}^{n\times m}$ and $B \in \mathbb{R}^{m\times n}$, then

$$tr(AB) = tr(BA).$$

3.3 Closed-Loop Error System

The open-loop error system for the mass can be obtained by multiplying (14) by m and then taking its time derivative as

$$m\dot{r}_m = k_s(x_m - x_0) - \Lambda\lambda\delta^n - \Lambda b\dot{\delta}\delta^n + \chi - m\gamma_1^2 e_m - m\gamma_2 k_1 r_m, \tag{23}$$

where $\chi(e_m, r_m, e_f, t) \in \mathbb{R}$ is an auxiliary term defined as

$$\chi \triangleq m\gamma_1 r_m + m\gamma_2^2 e_m - (m\gamma_1\gamma_2 + m\gamma_2\gamma_3)e_f. \tag{24}$$

The auxiliary expression $\chi(e_m, r_m, e_f, t)$ defined in (24) can be upper bounded as

$$\chi \leq \zeta \|z\|, \tag{25}$$

where $\zeta \in \mathbb{R}$ is a known positive constant, and $z(t) \in \mathbb{R}^3$ is defined as

$$z \triangleq \left[r_m \; e_m \; e_f \right]^T. \tag{26}$$

4

The expression in (23) can be written as

$$m\dot{r}_m = f_1 - \Lambda b\dot{\delta}\delta^n + \chi - m\gamma_1^2 e_m - m\gamma_2 k_1 r_m, \tag{27}$$

where the function $f_1(t) \in \mathbb{R}$ containing the uncertain spring and environment stiffness constants, is defined as

$$f_1 \triangleq k_s(x_m - x_0) - \Lambda\lambda\delta^n. \tag{28}$$

The auxillary function in (28) can be represented by a three layer NN as

$$f_1 = W_1^T \sigma_1\left(V_1^T x_1\right) + \varepsilon_m(x_1), \tag{29}$$

where the NN input $x_1(t) \in \mathbb{R}^3$ is defined as $x_1 \triangleq [1,\, x_m,\, \Lambda\delta]^T$, $W_1 \in \mathbb{R}^{(N_{m2}+1)\times 1}$ and $V_1 \in \mathbb{R}^{3\times N_{m2}}$ are ideal NN weights, and $N_{m2} \in \mathbb{R}$ denotes the number of hidden layer neurons of the NN. Since the open loop error expression for the mass in (27) doesn't have an actual control input, a virtual control input, $\dot{x}_{rd1}(t)$, is introduced by adding and subtracting $(1-\Lambda b\delta^n)\dot{x}_{rd1}$ to (27) as

$$\begin{aligned} m\dot{r}_m = {} & f_1 - \Lambda b\dot{\delta}\delta^n + \chi - m\gamma_1^2 e_m - m\gamma_2 k_1 r_m \\ & + (1-\Lambda b\delta^n)\dot{x}_{rd1} - (1-\Lambda b\delta^n)\dot{x}_{rd1}. \end{aligned} \tag{30}$$

To facilitate the subsequent backstepping-based design, the virtual control input to the unactuated mass-spring system, $\dot{x}_{rd1}(t)$ is designed as

$$\dot{x}_{rd1} = \hat{f}_1, \tag{31}$$

Also, $x_{rd2} = \rho$ where $\rho \in \mathbb{R}$ is an appropriate positive constant, selected so the robot will impact the mass-spring system. In (31), $\hat{f}_1(t) \in \mathbb{R}$ is the estimate for $f_1(t)$ and is defined as

$$\hat{f}_1 \triangleq \hat{W}_1^T \sigma_1(\hat{V}_1^T x_1), \tag{32}$$

where $\hat{W}_1(t) \in \mathbb{R}^{(N_{m2}+1)\times 1}$ and $\hat{V}_1(t) \in \mathbb{R}^{3\times N_{m2}}$ are the estimates of the ideal weights, which are updated based on the subsequent stability analysis as

$$\begin{aligned} \dot{\hat{W}}_1 &= \Gamma_{w1}\hat{\sigma}_1 r_m - \Gamma_{w1}\hat{\sigma}_1' \hat{V}_1^T x_1 r_m, \\ \dot{\hat{V}}_1 &= \Gamma_{v1} x_1 \hat{W}_1^T \hat{\sigma}_1' r_m, \end{aligned} \tag{33}$$

where $\Gamma_{w1} \in \mathbb{R}^{(N_{m2}+1)\times(N_{m2}+1)}$, $\Gamma_{v1} \in \mathbb{R}^{3\times 3}$ are constant, positive definite, symmetric gain matrices. The estimates for the NN weights in (33) are generated on-line (there is no off-line learning phase). The closed loop error system for the mass can be developed by substituting (31) into (30) and using (13) as

$$\begin{aligned} m\dot{r}_m = {} & f_1 - \hat{f}_1 + \Lambda b\delta^n \dot{e}_{r1} - \Lambda b\delta^n \dot{e}_m + \chi \\ & - m\gamma_1^2 e_m - m\gamma_2 k_1 r_m + (1-\Lambda b\delta^n)\dot{x}_{rd1}. \end{aligned} \tag{34}$$

Using (29) and (32), the expression in (34) can be written as

$$\begin{aligned} m\dot{r}_m = {} & W_1^T \sigma_1\left(V_1^T x_1\right) - \hat{W}_1^T \sigma_1(\hat{V}_1^T x_1) + \varepsilon_m(x_1) \\ & + \Lambda b\delta^n \dot{e}_{r1} - \Lambda b\delta^n \dot{e}_m + \chi - m\gamma_1^2 e_m \\ & - m\gamma_2 k_1 r_m + (1-\Lambda b\delta^n)\dot{x}_{rd1}. \end{aligned} \tag{35}$$

Adding and subtracting $W_1^T\hat{\sigma}_1 + \hat{W}_1^T\tilde{\sigma}_1$ to (35), and then using the Taylor series approximation in (20), the following expression for the closed loop mass error system can be obtained

$$\begin{aligned} m\dot{r}_m = {} & \tilde{W}_1^T\hat{\sigma}_1 - \tilde{W}_1^T\hat{\sigma}_1'\hat{V}_1^T x_1 + \hat{W}_1^T\hat{\sigma}_1'\tilde{V}_1^T x_1 \\ & + w_1 - m\gamma_1^2 e_m - m\gamma_2 k_1 r_m, \end{aligned} \tag{36}$$

where the notations $\hat{\sigma}_1$ and $\tilde{\sigma}_1$ were introduced in (18), and $w_1(t) \in \mathbb{R}$ is defined as

$$\begin{aligned} w_1 = {} & \tilde{W}_1^T\hat{\sigma}_1' V_1^T x_1 + W_1^T O(\tilde{V}_1^T x_1)^2 + \varepsilon_m(x_1) \\ & + \Lambda b\delta^n \dot{e}_{r1} - \Lambda b\delta^n \dot{e}_m + \chi + (1-\Lambda b\delta^n)\dot{x}_{rd1}. \end{aligned} \tag{37}$$

It can be shown from Property 6, Property 7, and [25] that $w_1(t)$ can be bounded as

$$|w_1| \le c_{m1} + c_{m2}\|z\| + c_{m3}\|e_r\| + c_{m4}\|r_r\|, \tag{38}$$

where $c_{mi} \in \mathbb{R}$, $(i = 1,2,\ldots,4)$ are computable known positive constants. In (36), $k_1 \in \mathbb{R}$ is a positive constant control gain defined, based on the subsequent stability analysis, as

$$k_1 \triangleq \frac{1}{\underline{m}\gamma_2} + \frac{k_{n1}}{4\gamma_2} + \frac{1}{4\underline{m}\gamma_2}(k_{n2} + c_{m2}^2 k_{n3}) + \frac{1}{4\underline{m}\gamma_2}(c_{m3}^2 k_{n4} + c_{m4}^2 k_{n5}), \tag{39}$$

where $k_{ni} \in \mathbb{R}$, $(i = 1,2,\ldots,5)$ are positive constant nonlinear damping gains, and $\underline{m}$ and γ_2 are defined in (12) and (14).

The open-loop robot error system can be obtained by taking the time derivative of $r_r(t)$, premultiplying by the robot inertia matrix $M(x_r)$, and utilizing (1), (13), and (14) as

$$M\dot{r}_r = f_2 - Cr_r - F, \tag{40}$$

where the function $f_2(t) \in \mathbb{R}^2$, contains the uncertain robot and Hunt-Crossley model parameter, and is defined as

$$\begin{aligned} f_2 \triangleq {} & M\ddot{x}_{rd} + \alpha M\dot{e}_r + h + C\dot{x}_{rd} + \alpha C x_{rd} \\ & + \begin{bmatrix} \Lambda(\lambda\delta^n + b\dot{\delta}\delta^n) \\ 0 \end{bmatrix} - \alpha C x_r. \end{aligned} \tag{41}$$

By representing the function $f_2(t)$ by a NN, the expression in (40) can be written as

$$M\dot{r}_r = W_2^T \sigma_2\left(V_2^T x_2\right) + \varepsilon_r(x_2) - Cr_r - F, \tag{42}$$

where the NN input $x_2(t) \in \mathbb{R}^{13}$ is defined as $x_2(t) \triangleq [1,\, \Lambda\delta,\, x_r^T,\, x_{rd}^T,\, \dot{\delta},\, \dot{x}_r^T,\, \dot{x}_{rd}^T,\, \ddot{x}_{rd}^T]^T$, $W_2 \in \mathbb{R}^{(N_{r2}+1)\times 2}$ and $V_2 \in \mathbb{R}^{13\times N_{r2}}$ are ideal NN weights and $N_{r2} \in \mathbb{R}$ denotes the number of hidden layer neurons of the NN. An expression for $\ddot{x}_{rd1}(t)$ can be developed to illustrate that the second derivative of the desired trajectory is continuous and does not require acceleration measurements. Based on (42) and the subsequent stability analysis, the robot force control input is designed as

$$F = \hat{W}_2^T \sigma_2(\hat{V}_2^T x_2) + k_2 r_r + e_r, \tag{43}$$

where $k_2 \in \mathbb{R}$ is a constant positive control gain defined in (48), and $\hat{W}_2(t) \in \mathbb{R}^{(N_{r2}+1)\times 2}$ and $\hat{V}_2(t) \in \mathbb{R}^{13\times N_{r2}}$ are the estimates of the ideal weights, which are designed based on the subsequent stability analysis as

$$\begin{aligned}\dot{\hat{W}}_2 &= \Gamma_{w2}\hat{\sigma}_2 r_r^T - \Gamma_{w2}\hat{\sigma}_2' \hat{V}_2^T x_2 r_r^T, \\ \dot{\hat{V}}_2 &= \Gamma_{v2} x_2 r_r^T \hat{W}_2^T \hat{\sigma}_2',\end{aligned} \tag{44}$$

where $\Gamma_{w2} \in \mathbb{R}^{(N_{r2}+1)\times(N_{r2}+1)}$, $\Gamma_{v2} \in \mathbb{R}^{13\times 13}$ are constant, positive definite, symmetric gain matrices. Substituting (43) in (42) and following similar approach as in the mass error system in (34)-(36), the closed loop error system for the robot is obtained as

$$\begin{aligned}M\dot{r}_r = {} & \tilde{W}_2^T \hat{\sigma}_2 - \tilde{W}_2^T \hat{\sigma}_2' \hat{V}_2^T x_2 + \hat{W}_2^T \hat{\sigma}_2' \tilde{V}_2^T x_2 \\ & + w_2 - C r_r - k_2 r_r - e_r,\end{aligned} \tag{45}$$

where $w_2(t) \in \mathbb{R}^2$ is defined as

$$w_2 = \tilde{W}_2^T \hat{\sigma}_2' V_2^T x_2 + W_2^T O(\tilde{V}_2^T x_2)^2 + \varepsilon_r(x_2). \tag{46}$$

It can be shown from Property 6, Property 7 and [25] that $w_2(t)$ can be bounded as

$$\|w_2\| \le c_{r1} + c_{r2}\|z\| + c_{r3}\|e_r\| + c_{r4}\|r_r\|, \tag{47}$$

where $c_{ri} \in \mathbb{R}$, $(i = 1,2,...,4)$ are computable known positive constants. Now, k_2 can be defined, based on the subsequent stability analysis, as

$$k_2 \triangleq k_{m1} + \frac{1}{4}(k_{m2} + c_{r2}^2 k_{m3}) + \frac{1}{4}(c_{r3}^2 k_{m4}), \tag{48}$$

where $k_{mi} \in \mathbb{R}$, $(i = 1,2,...,4)$ are positive constant nonlinear damping gains.

4 Stability Analysis

Theorem: The controller given by (31), (33), (43), and (44) ensures uniformly ultimately bounded regulation of the MSR system in the sense that

$$|e_m(t)|, \ \|e_r(t)\| \to \varepsilon_0 \exp(-\varepsilon_1 t) + \varepsilon_2 \tag{49}$$

provided k_{n2} and k_{m2} are chosen sufficiently large and the control gains are selected according to the sufficient gain conditions

$$\begin{aligned} k_{n1} &> \frac{\gamma_1^2 k_1^2}{\gamma_3} \\ k_{m1} &> c_{r4} + \frac{1}{k_{n5}} \\ \frac{1}{k_{n4}} + \frac{1}{k_{m4}} &< \alpha \\ \frac{1}{k_{n3}} + \frac{1}{k_{m3}} &< \nu, \end{aligned} \tag{50}$$

where ε_0, ε_1, $\varepsilon_2 \in \mathbb{R}$ denote positive constants; the control gains k_{ni} and k_{mi} are defined in (39) and (48) respectively; c_{r4} is defined in (46); α is defined in (14) and ν is a known bounding constant (see subsequent stability analysis).

Proof: Let $V(t) \in \mathbb{R}$ denote a non-negative, radially unbounded function (i.e., a Lyapunov function candidate) defined as

$$\begin{aligned} V = {} & \frac{1}{2} r_r^T M r_r + \frac{1}{2} e_r^T e_r \\ & + \frac{1}{2} tr(\tilde{W}_1^T \Gamma_{w1}^{-1} \tilde{W}_1) + \frac{1}{2} tr(\tilde{V}_1^T \Gamma_{v1}^{-1} \tilde{V}_1) \\ & + \frac{1}{2} tr(\tilde{W}_2^T \Gamma_{w2}^{-1} \tilde{W}_2) + \frac{1}{2} tr(\tilde{V}_2^T \Gamma_{v2}^{-1} \tilde{V}_2) \\ & + \frac{1}{2} m r_m^2 + \frac{1}{2}\gamma_1^2 m e_f^2 + \frac{1}{2}\gamma_1^2 m e_m^2. \end{aligned} \tag{51}$$

It follows directly from the bounds given in (7), (21), and Property 7, that $V(t)$ can be upper and lower bounded as

$$\lambda_1 \|y\|^2 \le V(t) \le \lambda_2 \|y\|^2 + \theta, \tag{52}$$

where λ_1, λ_2, $\theta \in \mathbb{R}$ are known positive bounding constants, and $y(t) \in \mathbb{R}^7$ is defined as

$$y \triangleq \left[r_r^T \ e_r^T \ z^T \right]^T. \tag{53}$$

The time derivative of $V(t)$ in (51) can be determined as

$$\begin{aligned} \dot{V} = {} & r_r^T M \dot{r}_r + \frac{1}{2} r_r^T \dot{M} r_r + e_r^T \dot{e}_r \\ & - tr(\tilde{W}_1^T \Gamma_{w1}^{-1} \dot{\hat{W}}_1) - tr(\tilde{V}_1^T \Gamma_{v1}^{-1} \dot{\hat{V}}_1) \\ & - tr(\tilde{W}_2^T \Gamma_{w2}^{-1} \dot{\hat{W}}_2) - tr(\tilde{V}_2^T \Gamma_{v2}^{-1} \dot{\hat{V}}_2) \\ & + r_m m \dot{r}_m + \gamma_1^2 m e_f \dot{e}_f + \gamma_1^2 m e_m \dot{e}_m. \end{aligned} \tag{54}$$

After using (8), (12), (14), (15), Property 10, (33), (36), (38), (39), (44), (45), (47), and (48), an upper bound for the expression in (54) can be determined as

$$
\begin{aligned}
\dot{V} \leq & -(k_{m1}-c_{r4})\|r_r\|^2-\alpha\|e_r\|^2-\gamma_1^3\underline{m}e_m^2-\gamma_3\gamma_1^2 me_f^2-r_m^2 \\
& -\left[\frac{1}{4}mk_{n1}r_m^2-\gamma_1^2 mk_1|r_m||e_f|\right]-\left[\frac{1}{4}k_{n2}r_m^2-c_{m1}|r_m|\right] \\
& -\left[\frac{1}{4}c_{m4}^2k_{n5}r_m^2-c_{m4}\|r_r\||r_m|\right]-\left[\frac{1}{4}k_{m2}\|r_r\|^2-c_{r1}\|r_r\|\right] \\
& -\left[\frac{1}{4}c_{m2}^2k_{n3}r_m^2-c_{m2}\|z\||r_m|\right] \\
& -\left[\frac{1}{4}c_{m3}^2k_{n4}r_m^2-c_{m3}\|e_r\||r_m|\right] \\
& -\left[\frac{1}{4}c_{r2}^2k_{m3}\|r_r\|^2-c_{r2}\|z\|\|r_r\|\right] \\
& -\left[\frac{1}{4}c_{r3}^2k_{m4}\|r_r\|^2-c_{r3}\|e_r\|\|r_r\|\right]. \qquad (55)
\end{aligned}
$$

Completing the squares on the bracketed terms, and using (50), the following expression is obtained

$$
\begin{aligned}
\dot{V} \leq & -\left(k_{m1}-c_{r4}-\frac{1}{k_{n5}}\right)\|r_r\|^2 \qquad (56) \\
& -\left(\alpha-\frac{1}{k_{n4}}-\frac{1}{k_{m4}}\right)\|e_r\|^2 \\
& -\left(\nu-\frac{1}{k_{n3}}-\frac{1}{k_{m3}}\right)\|z\|^2+\frac{c_{m1}^2}{k_{n2}}+\frac{c_{r1}^2}{k_{m2}},
\end{aligned}
$$

where $\nu \in \mathbb{R}$ is defined as

$$\nu \triangleq \min\left\{\underline{m}\gamma_1^3, \underline{m}\left(\gamma_3\gamma_1^2-\frac{\gamma_1^4k_1^2}{k_{n1}}\right), 1\right\} \qquad (57)$$

The expression in (56) can be further upper bounded as

$$\dot{V} \leq -\beta\|y\|^2+\frac{c_{m1}^2}{k_{n2}}+\frac{c_{r1}^2}{k_{m2}}, \qquad (58)$$

where $\beta \in \mathbb{R}$ is defined as

$$
\begin{aligned}
\beta \triangleq \min & \left\{\left(k_{m1}-c_{r4}-\frac{1}{k_{n5}}\right), \left(\alpha-\frac{1}{k_{n4}}-\frac{1}{k_{m4}}\right),\right. \\
& \left.\left(\nu-\frac{1}{k_{n3}}-\frac{1}{k_{m3}}\right)\right\}.
\end{aligned}
$$

Since the inequality in (52) can be utilized to lower bound $\|y(t)\|^2$ as

$$\|y\|^2 \geq \frac{V(t)}{\lambda_2}-\frac{\theta}{\lambda_2}, \qquad (59)$$

the inequality in (58) can be expressed as

$$\dot{V}(t) \leq -\frac{\beta}{\lambda_2}V(t)+\varepsilon_x, \qquad (60)$$

where $\varepsilon_x \in \mathbb{R}$ is a positive constant defined as

$$\varepsilon_x \triangleq +\frac{c_{m1}^2}{k_{n2}}+\frac{c_{r1}^2}{k_{m2}}+\frac{\beta\theta}{\lambda_2}. \qquad (61)$$

The linear differential inequality in (60) can be solved as

$$V(t) \leq V(0)e^{(-\frac{\beta}{\lambda_2})t}+\varepsilon_x\frac{\lambda_2}{\beta}\left[1-e^{(-\frac{\beta}{\lambda_2})t}\right]. \qquad (62)$$

The inequalities in (52) can now be used along with (61) and (62) to conclude that

$$
\begin{aligned}
\|y\|^2 \leq & \left[\frac{\lambda_2\|y(0)\|^2+\theta}{\lambda_1}\right]e^{(-\frac{\beta}{\lambda_2})t} \qquad (63) \\
& +\left[\left(+\frac{c_{m1}^2}{k_{n2}}+\frac{c_{r1}^2}{k_{m2}}\right)\frac{\lambda_2}{\lambda_1\beta}+\frac{\theta}{\lambda_1}\right]. \qquad (64)
\end{aligned}
$$

Provided the gain conditions in (50) are satisfied, and k_{n2} and k_{m2} are chosen sufficiently large, the definitions in (26) and (53), and the expressions in (62) and (63) can be used to prove that $r_r(t)$, $e_r(t)$, $r_m(t)$, $e_m(t)$, $e_f(t) \in \mathcal{L}_\infty$. Since $x_r(t) \in \mathcal{L}_\infty$ from Assumption 1 and $e_r(t) \in \mathcal{L}_\infty$, it can be shown that $x_{rd1}(t) \in \mathcal{L}_\infty$. Since $r_m(t)$, $e_m(t)$, $e_f(t) \in \mathcal{L}_\infty$, it can be shown from (14) that $\dot{e}_m(t) \in \mathcal{L}_\infty$, and hence $\dot{x}_m(t) \in \mathcal{L}_\infty$ from (13). Since $\hat{W}_1(t)$, $\hat{V}_1(t)$, $\sigma_1(\cdot) \in \mathcal{L}_\infty$ from Property 8 and Property 9, it can be shown from (31) that $\dot{x}_{rd1}(t) \in \mathcal{L}_\infty$. Since $r_r(t) \in \mathcal{L}_\infty$, linear analysis methods can be used to prove that $\dot{e}_r(t) \in \mathcal{L}_\infty$. Because $\dot{e}_r(t)$, $\dot{x}_{rd1}(t) \in \mathcal{L}_\infty$, (13) can be used to show that $\dot{x}_{r1}(t) \in \mathcal{L}_\infty$. Since $x_{r1}(t), x_m(t), \dot{x}_{r1}(t), \dot{x}_m(t)$, $r_m(t) \in \mathcal{L}_\infty$, it can be shown that $\ddot{x}_{rd1}(t) \in \mathcal{L}_\infty$. Since $\hat{W}_2(t)$, $\hat{V}_2(t)$, $\sigma_2(\cdot) \in \mathcal{L}_\infty$ from Property 7 and Property 8, it can be shown from (43), that the control input $F \in \mathcal{L}_\infty$. The result in (49) can be directly obtained from (63).

5 Conclusion

In this paper, a continuous NN-based controller is used to control a parametrically uncertain robot as it transitions from non-contact to contact state with an uncertain non-parametric Hunt-Crossley viscoelastic material so that the coupled system converges to a desired setpoint. This use of NN-based estimation in this paper helps us overcome the restriction in our previous work, where the Hertzian compliance coefficient was required to be known. A contribution of the work is that a continuous controller is used to obtain a uniformly ultimately bounded regulation result, and the developed controller does not require force or acceleration measurements. An experimental testbed is currently being developed with a two link direct drive robot that will collide with a viscoelastic human tissue phantom to test the performance of the developed controller.

REFERENCES

[1] S Jezernik, M Morari, "Controlling the human-robot interaction for robotic rehabilitation of locomotion", *7th International Workshop on Advanced Motion Control*, (2002).

[2] Cozens, J.A., "Robotic assistance of an active upper limb exercise in neurologically impaired patients", *IEEE Transactions on Rehabilitation Engineering*, (1999).

[3] Okamura, A.M. Smaby, N. Cutkosky, M.R., "An overview of dexterous manipulation", *IEEE International Conference on Robotics and Automation*, (2000).

[4] H. Hertz, Miscellaneous papers. In: H. Hertz, *Macmillan*, London (1896).

[5] W. Goldsmith, *Impact: The Theory and Physical Behavior of Colliding Solids*, (1960).

[6] S. Dubowsky and F. Freudenstein, "Dynamic analysis of mechanical systems with clearances—-Part 1: Formation of dynamical model", *Journal of Engineering for Industry* 93, pp. 305–309, (1971).

[7] K.H. Hunt and F.R.E. Crossley, "Coefficient of restitution interpreted as damping in vibroimpact", *Journal of Applied Mechanics* 42, Series E , pp. 440–445, (1975).

[8] G. Gilardi and I. Sharf, "Literature survey of contact dynamics modelling", *Mechanism and Machine Theory*, Volume 37, Issue 10, Pages 1213-1239, (2002).

[9] D.W. Marhefka and D.E. Orin, "A compliant contact model with nonlinear damping for simulation of robotic systems", *IEEE Transactions on Systems, Man, and Cybernetics*-Part A: Systems and Humans , pp. 566–572, (1999).

[10] H.M. Lankarani and P.E. Nikravesh, "A contact force model with hysteresis damping for impact analysis of multi-body systems", *Journal of Mechanical Design* 112 , pp. 369–376, (1990).

[11] N Diolaiti, C Melchiorri, S Stramigioli, "Contact impedance estimation for robotic systems", *Proceedings of IEEE/RSJ International Conference on Intelligent Robots and Systems*, (2004).

[12] Hogan, N, "Impedance control: An approach to manipulation: Parts I, II, and III", *J. Dynamic Sys. Measurement Control* 107:1-24, (1985).

[13] Youcef-Toumi, K. and Gutz, D, "Impact and force control", *Proceedings of the IEEE Conference on Robotics and Automation*, pp. 410-416, (1989)

[14] Raibert, M., and Craig, J., "Hybrid position/force control of manipulators", *ASME J. of Dyn. Sys. Meas.Control*,102(2):126-133 (1981).

[15] A. Tornambe, "Modeling and Control of Impact in Mechanical Systems: Theory and Experimental Results", *IEEE Transactions on Automatic Control*, Vol. 44, No. 2, pp. 294-309, (1999).

[16] R. Volpe and P. Khosla, "A Theoretical and Experimental Investigation of Impact Control for Manipulators", *International Journal of Robotics Research*, Vol. 12, No. 4, pp. 670-683, (1994).

[17] K. Dupree, W. E. Dixon, G. Hu, and C. Liang, "Lyapunov-Based Control of a Robot and Mass-Spring System Undergoing An Impact Collision", *Proceedings of the IEEE American Control Conference,* Minneapolis, MN, pp. 3241-3246, (2006).

[18] K. Dupree, C. Liang, G. Hu, and W. E. Dixon, "Global Adaptive Lyapunov-Based Control of a Robot and Mass-Spring System Undergoing an Impact Collision", IEEE Transactions on Systems, Man and Cybernetics, to appear.

[19] C. Liang, S. Bhasin, K. Dupree, and W. E. Dixon, "An Impact Force Limiting Adaptive Controller for a Robotic System Undergoing a Non-Contact to Contact Transition", *Proceedings of the IEEE Conference on Decision and Controls*, New Orleans, LA, (2007).

[20] S. Bhasin, K. Dupree, Z. D. Wilcox and W. E. Dixon, "Adaptive Control of a Robotic System Undergoing a Non-Contact to Contact Transition with a Viscoelastic Environment", *IEEE Conference on Decision and Control,* (2008), submitted.

[21] S Faik, H Witteman, "Modeling of Impact Dynamics: A Literature Survey", *Proceedings of international ADAMS user conference,* (2000).

[22] H Wang, K.H. Low, M.Y. Wang, "Reference Trajectory Generation for Force Tracking Impedance Control by Using Neural Network-based Environment Estimation", *IEEE Conference on Robotics, Automation and Mechatronics*, (2006).

[23] F. L. Lewis, "Nonlinear Network Structures for Feedback Control," *Asian Journal of Control*, Vol. 1, No. 4, pp. 205-228, 1999.

[24] F. L. Lewis, J. Campos, and R. Selmic, *Neuro-Fuzzy Control of Industrial Systems with Actuator Nonlinearities*, SIAM, PA, 2002.

[25] F. L. Lewis, A. Yesildirek, and K. Liu, "Multilayer neural-net robot controller: structure and stability proofs", IEEE Trans. Neural Networks, (1996)

[26] P. M. Patre, W. MacKunis, K Kaiser, W. E. Dixon, "Asymptotic Tracking for Uncertain Dynamic Systems via a Multilayer NN Feedforward and RISE Feedback Control Structure", *American Control Conference*, (2007).

